NANO LETTERS
Letter
Cite This: Nano Lett. 2018, 18, 6392−6396
pubs.acs.org/NanoLett

Enhanced Boiling Heat Transfer using Self-Actuated Nanobimorphs

Sangwoo Shin,[†,▽] Geehong Choi,[‡,▽] Bhargav Rallabandi,[§,∥] Donghwi Lee,[‡] Dong Il Shim,[‡] Beom Seok Kim,[⊥] Kyung Min Kim,[#] and Hyung Hee Cho*[,‡]

[†]Department of Mechanical Engineering, University of Hawaii at Manoa, Honolulu, Hawaii 96822, United States
[‡]Department of Mechanical Engineering, Yonsei University, Seoul 03722, Republic of Korea
[§]Department of Mechanical and Aerospace Engineering, Princeton University, Princeton, New Jersey 08544, United States
[∥]Department of Mechanical Engineering, University of California Riverside, Riverside, California 92521, United States
[⊥]DEMO Technology Division, National Fusion Research Institute, Daejeon 34133, Republic of Korea
[#]Korea District Heating Corporation, Seoul 13585, Republic of Korea

Supporting Information

ABSTRACT: We present a new concept of a structured surface for enhanced boiling heat transfer that is capable of self-adapting to the local thermal conditions. An array of freestanding nanoscale bimorphs, a structure that consists of two adjoining materials with a large thermal expansion mismatch, is able to deform under local temperature change. Such a surface gradually deforms as the nucleate boiling progresses due to the increase in the wall superheat. The deformation caused by the heated surface is shown to be favorable for boiling heat transfer, leading to about 10% of increase in the critical heat flux compared to a regular nanowire surface. A recently developed theoretical model that accounts for the critical instability wavelength of the vapor film and the capillary wicking force successfully describes the critical heat flux enhancement for the nanobimorph surface with a good quantitative agreement.

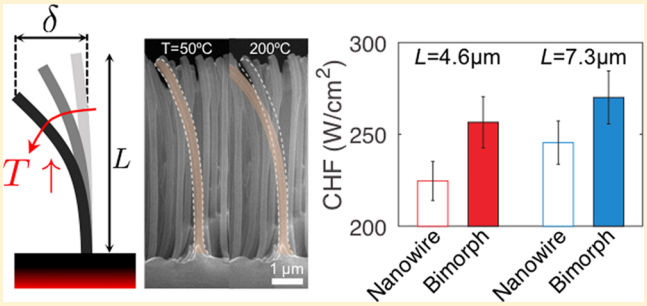

KEYWORDS: *Nanowires, bimorph, phase-change, boiling heat transfer, critical heat flux*

One of the most important factors that determines the efficacy of boiling heat transfer is the critical heat flux (CHF), which refers to the threshold heat flux above which the surface dry-out occurs.[1] CHF determines the practical operating limit for cooling applications because the surface will eventually experience overheating followed by meltdown beyond this point due to the reduced heat transfer, as witnessed from the recent disaster in Fukushima nuclear power plant.[2] In this regard, extensive efforts have been put into increasing the CHF; to date, one of the most effective ways of enhancing the CHF is by roughening the surface with micro/nanostructures, for example, nanowires.[3−8] An array of nanowires exhibits extremely high surface roughness, leading to increased number of nucleation sites. Moreover, the presence of nanowires enables enhanced wetting and capillary pumping due to the narrow pore spaces, allowing significant enhancement in CHF by more than 100% compared to a smooth surface.[3−7]

Another recent approach of extending the CHF is by manipulating the motion of nucleated bubbles. One way is to induce lateral bubble motion by using an asymmetric structure.[9,10] Another recent approach is to impinge jets near the boiling site, which drives an upward flow above the heated area that can carry away the bubbles at a faster rate.[11,12] These set of studies highlight that the fast ebullition of a large number of nucleated bubbles is critical for enhancing the CHF.

In this paper, we propose a new concept of nanostructure that further enhances CHF compared with a nanowire surface, that is, one that produces mechanical actuation in response to the surface temperature. Here, we use an array of nanoscale freestanding bimorphs; a bimorph refers to a structure that consists of two adjecent materials with a large thermal expansion coefficient difference in contact and hence deforms under ambient temperature changes.[13] As the nucleate boiling progresses, the increasing surface temperature actuates the deformation of the bimorph array. We show that such a deformation creates a structure that is favorable for promoting bubble departure and capillary wicking, thus extending the CHF.

A schematic illustrating the deformation of a nanobimorph due to the change in the surface temperature is presented in Figure 1a. An array of nanoscale bimorphs is placed vertically on a heated surface where the bimorphs deform as the surface is heated. This deformation effectively increases the surface

Received: July 5, 2018
Revised: August 19, 2018
Published: August 31, 2018

DOI: 10.1021/acs.nanolett.8b02747
Nano Lett. 2018, 18, 6392−6396

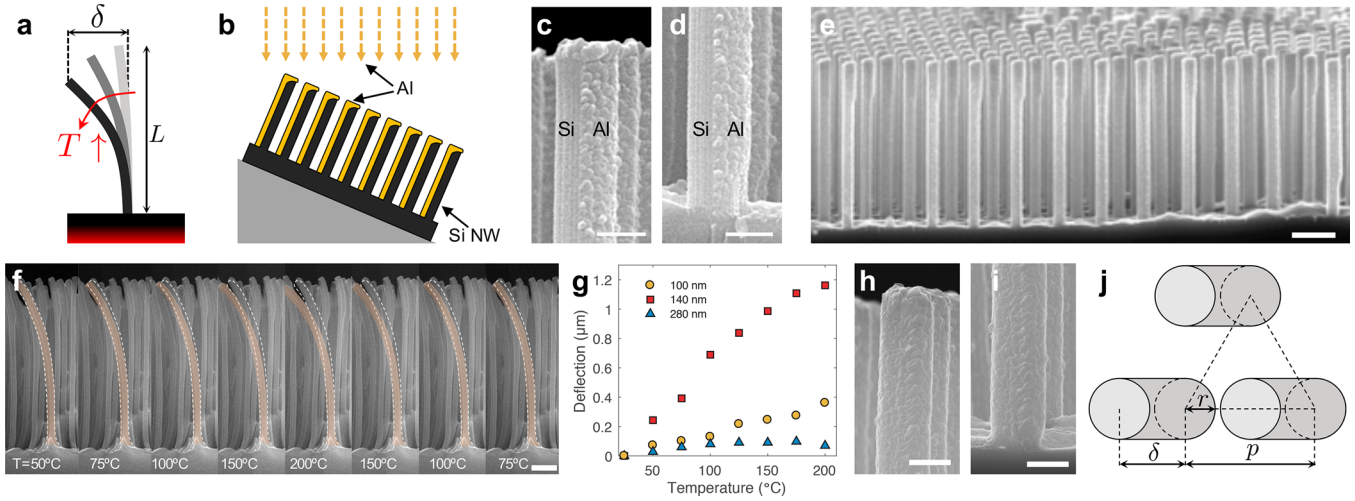

Figure 1. Self-actuating nanobimorph arrays. (a) A schematic illustrating the deformation of a bimorph due to the change in the surface temperature. (b) An ordered array of bimorphs is achieved by depositing the metal layer on Si nanowires in an oblique angle. (c–e) SEM images show that the Al layer is coated evenly from the top (c) to the bottom (d) of the nanowire on a large area (e). (f,g) Deformation of the bimorph upon exposure to different temperatures. (f) The in situ SEM imaging shows reversible bending of the bimorph with minimum hysteresis. The frontmost bimorph was false-colored for a guide to the eye. (g) The degree of the deformation depends on the thickness of the Al layer. (h,i) SEM images of Si/Al "core–shell" nanowire that has Al deposited on the both sides of the nanowire. (j) Illustration of an array of deformed bimorph seen from the top. Scale bars are 500 nm for (c,d,h,i) and 1 μm for (e,f).

fraction (ϕ_s, ratio of the projected cross-sectional area of the structure and the substrate area). On the basis of the recent theoretical prediction by Quan et al.,[14] such an increase in the surface fraction effectively reduces the critical instability wavelength of the vapor film and increases the capillary wicking, both of which lead to enhanced CHF. We confirm experimentally that this is indeed valid and shows that the CHF of a nanobimorph surface can further exceed that of the nanowire surface, reaching up to 271 W/cm^2 for stagnant water at a saturated condition.

To achieve a uniform array of nanobimorphs on a large area, we deposit metal layer on the already synthesized nanowires at an oblique angle (Figure 1b). Further fabrication details can be found in the Supporting Information. This process allows easy fabrication of nanobimorphs with well-controlled thickness, from the tip of the nanowire (Figure 1c) to the bottom (Figure 1d) on a large area (Figure 1e). The deposited metal was chosen to maximize the mismatch of the thermal expansion coefficient α, for which we choose aluminum ($\alpha_{Si} \approx 3.3 \times 10^{-6}$ K^{-1},[15] $\alpha_{Al} \approx 23.8 \times 10^{-6}$ K^{-1}[16]). Si nanowire as a base material ensures fast thermal response that can rapidly adapt to the temperature change due to its short thermal diffusion time scale, which is ≈1 ns for current geometry.

The deformation of the fabricated bimorph under varying temperature is presented in Figure 1f. The in situ scanning electron microscope (SEM) images clearly show that reversible bending of the bimorph is observed upon exposure to different temperature conditions. The deformation also shows minimum hysteresis, which can be important for a long-term operation. The bending also depends on the thickness of the metal deposit as it shows an optimal thickness of ≈140 nm for the maximum bending (Figure 1g). As shown in Figure 1g, the deformation increases linearly with temperature, which can be predicted from a theoretical analysis where we obtain the temperature-dependent deformation as

$$\delta \approx \frac{L^2 \Delta T \Delta \alpha}{4r} \quad (1)$$

Here, L is the length of the bimorph, ΔT is the temperature change, $\Delta\alpha$ is the difference in the thermal expansion coefficients between the two adjoining materials, and r is the radius of the bimorph. A detailed derivation of eq 1 is provided in the Supporting Information. For example, inserting realistic numbers for the nanobimorphs shown in Figure 1f, that is, $L \approx$ 15 μm, $r \approx 0.25$ μm, the theory yields $\delta \approx 0.59$ μm at $\Delta T =$ 100 K, which agrees reasonably with the measured value ($\delta \approx$ 0.82 μm).

For control experiments, we have further fabricated nanobimorphs with chromium as a side layer, which has similar thermal expansion coefficient as silicon ($\alpha_{Cr} \approx 4.9 \times 10^{-6}$ K^{-1}[17]), and "core–shell" nanowires that has aluminum deposited on the both sides of the nanowire such that it has a geometrical symmetry (Figure 1h,i). These surfaces exhibit similar geometries and surface properties to those of the Si/Al nanobimorph surface but do not undergo deformation upon temperature change.

With the fabricated surfaces, we conduct pool boiling experiments using water as a working fluid. The boiling curves (i.e., heat flux versus wall superheat) at saturated condition (pool temperature = 100°C) are presented in Figure 2. Regardless of the length of the nanobimorphs, there is a clear tendency for the Si/Al nanobimorphs to exhibit higher CHF than the corresponding bare Si nanowires (Figure 2a). Furthermore, enhanced CHF is only observed for Si/Al nanobimorphs whereas Si/Cr nanobimorph and Si/Al core–shell nanowire do not show any appreciable enhancement in CHF over the bare nanowires (Figure 2b).

With a deposition of thin aluminum film only on one side of the nanowire, we observe CHF up to 271 W/cm^2, which is significantly larger that that of bare silicon surface (≈88 W/cm^2) and bare silicon nanowire (≈245 W/cm^2). Considering that a nanowire structure is regarded as a surface that exhibits the highest CHF in pool boiling among various types of micro/nanostructured surfaces,[8,18,19] this additional stretch in CHF can be particularly important in cooling of high heat flux

DOI: 10.1021/acs.nanolett.8b02747
Nano Lett. 2018, 18, 6392–6396

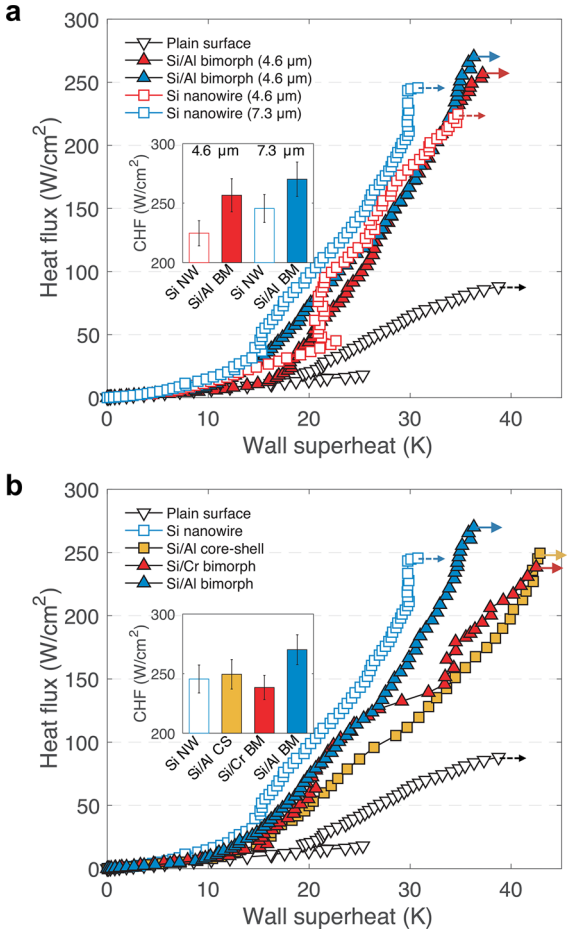

Figure 2. Bimorph structures show highest CHF among all other surfaces. (a,b) Boiling curves for the nanostructures with (a) different lengths and (b) different configurations/compositions. The inset represents the CHF values for different surfaces. The arrows indicate CHF.

devices such as nuclear fuel rods or electronics as CHF represents a technical milestone in boiling heat transfer.[1]

The enhancement of CHF for the nanobimorph surface is unexpected since the presence of metal film is anticipated to be unfavorable for heat transfer due to a number of following reasons: First, the presence of metal films provides an additional thermal resistance to the heated surface. This argument is supported by the fact that the wall superheat for the nanostructured surfaces with additional metal films are all shown to be higher than the bare silicon nanowire surface (Figures 2a,b), implying reduced heat transfer. Second, the thermal emissivities of the deposited metal films are much lower than the host material ($\varepsilon_{Al} \approx 0.03$, $\varepsilon_{Cr} \approx 0.08$, $\varepsilon_{Si} \approx 0.7$),[20,21] thus reducing the radiative heat transfer. Lastly, the presence of the metal film reduces the wettability of the surface as confirmed by the contact angle and the capillary rise measurements presented in Figure 3.

The wettability is one of the most critical factors that determines the CHF, because a superhydrophilic surface supplemented by fast capillary wicking is believed to be the driving factor for high CHF in nanowire surfaces.[7,8] However, the measurement results in Figure 3 confirm that these effects are suppressed when additional metal films are present. In detail, the nanowire reduces the apparent contact angle of the surface and the angle further decreases with increasing

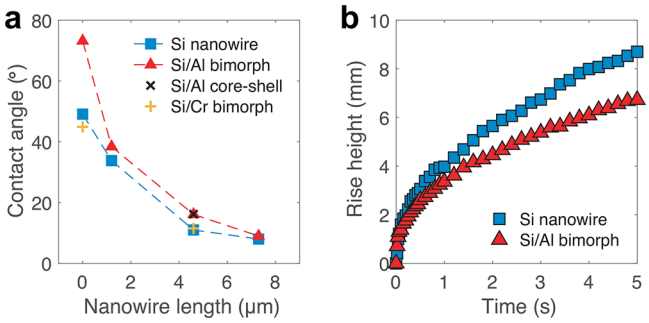

Figure 3. Bimorph structures show unfavorable wetting behavior for boiling heat transfer. (a) Static contact angle measurements of water droplets on different surfaces. Zero nanowire length indicate planar surfaces. (b) Capillary rise measurements for Si/Al bimorph and Si nanowire surfaces.

nanowire height (Figure 3a), which is consistent with theoretical prediction due to the larger degree of surface roughening.[22] However, it is observed that the presence of any additional metal films reduces the contact angle at any given nanowire length due to the altered surface property. Furthermore, the nanobimorph surface shows weaker capillary rise dynamics compared to the nanowire surface, indicating reduced capillary pumping of working fluid (Figure 3b). Thus, these experimental data suggest that the surface properties of the nanobimorph surface are disadvantageous for the boiling heat transfer. Then what causes the bimorph surfaces to exhibit higher CHF than any other surfaces?

Physically, the CHF renders a situation where the removal of the vapor near the surface due to the bubble ebullition is slower than the generation due to the bubble growth such that the surface is deficit of the working fluid.[1] In this regard, high bubbling frequency with small bubble departure diameter is favorable for higher CHF. Indeed, we observe that the nanobimorph surface exhibits faster bubbling frequency (Figure 4a) and smaller bubble diameter (Figure 4b) than the nanowire surface despite the aforementioned disadvantages, both of which are footprints of enhanced CHF.

We attribute such distinct dynamics to the deformation of the nanobimorphs driven by the local change in the surface temperature. While bubbling frequency is typically known to be constant across varying heat flux conditions within the nucleate boiling regime,[6] which is also shown for the planar and the nanowire surfaces in Figure 4a, the bubbling frequency for the nanobimorph surface is shown to be heat-flux-dependent, implying that the temperature-dependent bending of the bimorph structure is responsible for such dynamics. In addition, boiling experiments conducted at a subcooled condition (pool temperature = 90 °C) leads to a larger degree of CHF enhancement for the nanobiomorph surface compared to the nanowire surface (Figure 4c), further suggesting that the dynamics is related to the temperature difference.

As the bending of the nanobimorphs increases due to increased surface temperature, the effective solid fraction ϕ_s is increased, as sketched in Figure 1a,j. Because of the high area density of the nanobimorph array, a slight deformation can lead to large change in ϕ_s. For example, from geometrical calculations (Figure 1j), the surface fraction for a surface with deformed bimorphs can be expressed as $\phi_s = (2\pi r^2 + 4\delta r)/(\sqrt{3}p^2)$, where p is the distance between

DOI: 10.1021/acs.nanolett.8b02747
Nano Lett. 2018, 18, 6392−6396

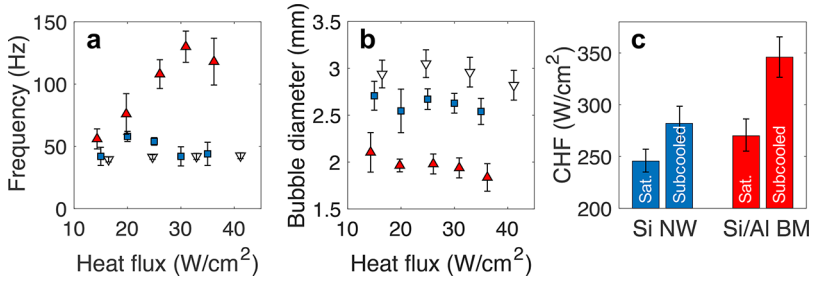

Figure 4. Bimorph structures show temperature dependent dynamics. (a) Bubbling frequencies, (b) bubble diameters, and (c) CHF values at saturated (pool temperature = 100°C) and subcooled (pool temperature = 90°C) conditions for various surfaces. Red triangles, blue squares, and white inverted triangles in (a,b) represent Si/Al nanobimorph, Si nanowire, and plain surface, respectively.

the bimorphs. Thus, a bimorph having a deformation of its own radius (i.e., $\delta = r$) leads to $2/\pi \approx 64\%$ enhancement in ϕ_s.

The consequence of increased ϕ_s is the reduction in the critical instability wavelength of the vapor film, which is the length scale corresponding to the bubble departure diameter. The critical wavelength λ_c of the vapor wave transmitted along the surface nanostructure was first modeled by Quan et al.[14] and scales with ϕ_s as $\lambda_c \sim (1 - \sqrt{\phi_s})^{1/2}$, which is in a qualititave agreement with the experimental observations in Figure 4b. Taking into account the reduced critical instability wavelength and the capillary wicking force, the CHF of a rough surface can be calculated from a force balance on a single vapor bubble and is given as

$$q_{CHF} = Kh_{fg}[\sigma_{lv} g \rho_v^2 (\rho_l - \rho_v)]^{1/4} \quad (2)$$

where h_{fg} is the latent heat, σ_{lv} is the surface tension of the liquid, g is the gravitational acceleration, and $\rho_{l,v}$ are, respectively, the density of liquid and vapor. Also, K is the dimensionless CHF given as

$$K = \left(\frac{1 + \cos\theta}{16}\right)\left[\frac{2}{\pi}(1 - \sqrt{\phi_s})^{-1/2}\left(\frac{R + \cos\theta}{1 + \cos\theta}\right) + \frac{\pi}{4}(1 - \sqrt{\phi_s})^{1/2}(1 + \cos\theta)\right] \quad (3)$$

where θ is the apparent contact angle of the boiling surface, and $R = 1 + 4\pi rL/(\sqrt{3}p^2)$ is the surface roughness. Equations 2 and 3 predict that increased ϕ_s leads to enhanced CHF due to the contribution of reduced critical wavelength and the enhanced capillary wicking.[14] Although the presence of a metal film reduces the wettability due to the changed surface property as shown in Figure 3, capillary wicking is anticipated to be enhanced as the bimorphs gradually deform since the bending provides more contact area for the wicking to occur, as evidenced from curved nanowires.[23]

Using eq 1, the surface fraction increases from $\phi_s = 0.04$–0.10 near the CHF ($T \approx 135$ °C) for the nanobimorph surface used in the pool boiling experiment shown in Figures 1e and 2a ($L \approx 7.3$ μm). Then, using eq 3 the CHF enhancement of the nanobimorph surface compared to the nanowire surface is calculated as ≈15.8%. This values is in a good agreement with the experimental observations in Figure 2, measured as ≈10.6%, which strengthens our argument that the increase in the solid fraction of the nanobimorph surface due to the thermally induced deformation leads to enhanced CHF.

In summary, we have fabricated an ordered nanobimorph surface that can deform under temperature change. The surface is self-responding to the ambient condition such that the deformation caused by the heated surface is favorable for pool boiling in terms of higher CHF. A recently developed theoretical model that accounts for the critical instability wavelength and the capillary wicking force successfully describes the CHF enhancement with a good quantitative agreement. The nanobimorph surface presented in this study is a proof of concept without any design optimization being conducted. However, the study suggests that even further CHF enhancement can be expected for a nanobimorph surface with a proper design such as higher packing density or larger thermal expansion mismatch (for example, Zn, In, and so forth), which are left for future studies.

■ ASSOCIATED CONTENT

Supporting Information

The Supporting Information is available free of charge on the ACS Publications website at DOI: 10.1021/acs.nanolett.8b02747.

Experimental methods on the nanobimorph fabrication, in situ scanning electron microscopy, boiling experiments, and theoretical derivation of the bending of nanobimorphs (PDF)

■ AUTHOR INFORMATION

Corresponding Author

*E-mail: hhcho@yonsei.ac.kr.

ORCID

Sangwoo Shin: 0000-0001-5618-8522
Beom Seok Kim: 0000-0002-1182-1141
Hyung Hee Cho: 0000-0001-5309-3798

Author Contributions

▽S.S. and G.C. contributed equally to this work.

Notes

The authors declare no competing financial interest.

■ ACKNOWLEDGMENTS

This work was supported by the Center for Advanced Meta-Materials (CAMM) funded by the Ministry of Science, ICT, and Future Planning as Global Frontier Project (CAMM-No. NRF-2014M3A6B3063716) and the Human Resources Development Program (No. 20174030201720) of the Korea Institute of Energy Technology Evaluation and Planning (KETEP) funded by the Korean Government's Ministry of Trade, Industry and Energy.

DOI: 10.1021/acs.nanolett.8b02747
Nano Lett. 2018, 18, 6392–6396

REFERENCES

(1) Carey, V. P. *Liquid-Vapor Phase-Change Phenomena*; Hemisphere, New York, 1992.
(2) Lee, S. W.; Kim, S. M.; Park, S. D.; Bang, I. C. *Int. J. Heat Mass Transfer* **2013**, *60*, 105−113.
(3) Chen, R.; Lu, M.-C.; Srinivasan, V.; Wang, Z.; Cho, H. H.; Majumdar, A. *Nano Lett.* **2009**, *9*, 548−553.
(4) Lu, M.-C.; Chen, R.; Srinivasan, V.; Carey, V. P.; Majumdar, A. *Int. J. Heat Mass Transfer* **2011**, *54*, 5359−5367.
(5) Shin, S.; Kim, B. S.; Choi, G.; Lee, H.; Cho, H. H. *Appl. Phys. Lett.* **2012**, *101*, 251909.
(6) Kim, B. S.; Shin, S.; Lee, D.; Choi, G.; Lee, H.; Kim, K. M.; Cho, H. H. *Int. J. Heat Mass Transfer* **2014**, *70*, 23−32.
(7) Kim, B. S.; Lee, H.; Shin, S.; Choi, G.; Cho, H. H. *Appl. Phys. Lett.* **2014**, *105*, 191601.
(8) Shim, D. I.; Choi, G.; Lee, N.; Kim, T.; Kim, B. S.; Cho, H. H. *ACS Appl. Mater. Interfaces* **2017**, *9*, 17595.
(9) Kandlikar, S. G. *Appl. Phys. Lett.* **2013**, *102*, 051611.
(10) Raghupathi, P. A.; Kandlikar, S. G. *Int. J. Heat Mass Transfer* **2016**, *95*, 824−832.
(11) Jaikumar, A.; Kandlikar, S. G. *Appl. Phys. Lett.* **2017**, *110*, 094107.
(12) Kandlikar, S. G. *J. Heat Transfer* **2016**, *138*, 021504.
(13) Lammel, G.; Schweizer, S.; Renaud, P. *Optical Microscanners and Microspectrometers using Thermal Bimorph Actuators*; Springer Science & Business Media, 2013; Vol. *14*.
(14) Quan, X.; Dong, L.; Cheng, P. *Int. J. Heat Mass Transfer* **2014**, *76*, 452−458.
(15) Watanabe, H.; Yamada, N.; Okaji, M. *Int. J. Thermophys.* **2004**, *25*, 221−236.
(16) Hidnert, P. *J. Franklin Inst.* **1925**, *199*, 539−541.
(17) Koumelis, C. N. *Physica Status Solidi A* **1973**, *19*, K65.
(18) Bhavnani, S.; Narayanan, V.; Qu, W.; Jensen, M.; Kandlikar, S.; Kim, J.; Thome, J. *Nanoscale Microscale Thermophys. Eng.* **2014**, *18*, 197−222.
(19) Mori, S.; Utaka, Y. *Int. J. Heat Mass Transfer* **2017**, *108*, 2534−2557.
(20) Haynes, W. M. *CRC Handbook of Chemistry and Physics*; CRC Press, 2014.
(21) Timans, P. J. *J. Appl. Phys.* **1993**, *74*, 6353−6364.
(22) Kim, B. S.; Shin, S.; Shin, S. J.; Kim, K. M.; Cho, H. H. *Langmuir* **2011**, *27*, 10148−10156.
(23) Mai, T. T.; Lai, C. Q.; Zheng, H.; Balasubramanian, K.; Leong, K. C.; Lee, P. S.; Lee, C.; Choi, W. K. *Langmuir* **2012**, *28*, 11465−11471.

DOI: 10.1021/acs.nanolett.8b02747
Nano Lett. 2018, 18, 6392−6396